Neural mechanisms of binocular correspondence in monkey visual area V4

Seiji Tanabe   Graduate School of Frontier Biosciences, Osaka University

Kazumasa Umeda   Graduate School of Engineering Science, Osaka University

Ichiro Fujita   Graduate School of Frontier Biosciences, Osaka University

Stereoscopic depth is visible when viewing a random-dot stereogram (RDS), but invisible when the RDS is binocularly anticorrelated. The visual system cannot find a globally consistent solution for matching the left and right eye images of an anticorrelated RDS. Neurons in the striate cortex (V1) respond to binocular disparity in an anticorrelated RDS as if they are signaling depth information. To fully account for the matching computation, we examined single-cell responses to dynamic RDSs of both normal (correlated) and anticorrelated, in extrastriate area V4 of the monkey visual cortex. Most V4 neurons attenuated their selectivity for disparity when the RDS was anticorrelated. The attenuation was greater than that reported for V1 cells. Our results suggest that responses to false matches between contrast-reversed patterns in the left and right eye images elicited in V1 are reduced by the stage of V4.

Introduction

The visual system uses binocular disparity to derive the depth of visual targets and reconstruct three-dimensional scenes. The underlying computation involves extracting a globally consistent match from numerous possible matches between the visual patterns projected to the left and right eyes (Julesz, 1971; Marr & Poggio, 1979). Due to the white noise characteristic of a dynamic random-dot stereogram (RDS), a shift in the depth direction is visible only with the stereoscopic system and invisible with a monocular system. Any disparity shift is masked in the monocular view, because a shift in the retinal image always accompanies a renewal of the dot pattern.

Examination of neuronal sensitivity to horizontal binocular disparity in dynamic RDSs is a legitimate test for a neural representation of stereoscopic depth. Disparity selective cells are found in various visual cortical areas of the monkey brain, from as early as the striate cortex (V1) to as high as the posterior parietal and the inferior temporal (IT) cortices (Poggio et al. 1985; Taira et al. 2000; Janssen et al. 2001). Although neural responses in V1 are selective for the disparity in a dynamic RDS (Poggio et al., 1985), they are not the direct neural correlate of stereoscopic depth perception. When the binocular correlation of an RDS is reversed (Figure 1), the stereo correspondence does not have a global-match solution, and the perception of a depth-plane is greatly diminished or abolished (Cogan et al., 1993). In contrast, although the tuning profile is inverted compared to the one obtained by a normal RDS, the disparity selectivity of V1 neurons is largely retained by the contrast-reversal (Ohzawa et al., 1990; Cumming & Parker, 1997). Due to their local filter-like characteristics, most V1 neurons respond to local false-matches that do not coherently constitute a plane lying in depth. Further

processing in extrastriate areas is thus required for the rejection of false-match solutions.

The majority of cells in the middle-temporal (MT/V5) and the medial superior temporal areas (MST) respond to disparity in an anticorrelated RDS (Krug et al., 2004; Takemura et al., 2001). Neither of these areas appears to be the site where the correspondence problem is solved. To examine the process of the false-match rejection, we studied the disparity tuning of neurons to dynamic RDSs in area V4. Disparity tunings were examined with both normal (correlated; cRDS) and anticorrelated RDSs (aRDS). Area V4 is involved in processing of form, wavelength, and texture (Van Essen & Gallant, 1994), as well as binocular disparity in solid-figure stereograms (Hinkle & Connor, 2001; Watanabe et al., 2002). The results of the present study are published in Tanabe et al. (2004).
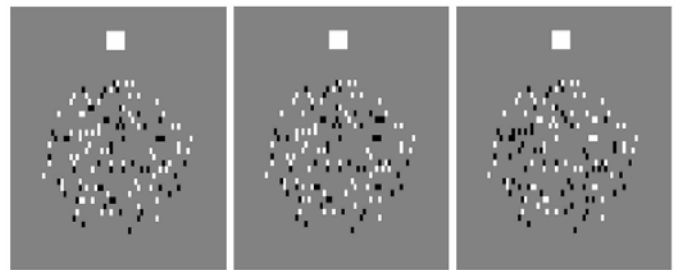
Figure 1. Random-dot stereogram (RDS). The left and center patches compose a normal RDS, and the center and right patches compose its anticorrelated version.

Method

Two female and one male Japanese macaque monkeys (*Macaca fuscata*) were used. Details of the surgical procedure have been published elsewhere (Uka et al. 2000). All surgical, experimental, and care protocols conformed to

the National Institutes of Health Guide for the Care and Use of Laboratory Animals (1996), and were approved by the Animal Experiment Committee of Osaka University.

Task and visual stimulation

Monkeys were seated with their head restrained in a primate chair. A computer display with liquid-crystal shutters for dichoptic presentation (NuVision 21MX, MacNaughton, Beaverton, OR) was set 57 cm away from the monkey's eyes. The display subtended 40° x 30° of the monkey's visual field. Both the left and right eye positions were monitored with magnetic search coils (MEL-25, Enzansi Kogyou, Tokyo, Japan). We trained the monkeys to perform a simple fixation task. During the 2 s of the trial period, the monkey had to maintain fixation within a fixation window of typically 1.4° x 1.4°, and the vergence window of ±0.5°. On successful trials, the monkey was rewarded with a drop of juice or water.

A dynamic RDS was presented for 1 s during the fixation period. The random-dot pattern was composed of 50% bright (3.5 cd/m^2) and 50% dark (0.4 cd/m^2) dots. All the dots had a size of 0.17° x 0.35° and were positioned following a uniform distribution of 26% density. The random-dot pattern was renewed every 5 frames (12 Hz). The background was a uniform field at mid-level luminance (1.5 cd/m^2). For visual stimulation, we illuminated only the red phosphors of the CRT display.

Single-cell electrophysiology

After the monkeys were sufficiently trained, a hole for electrode insertion was drilled through the skull inside the recording chamber that strode the region of area V4. On each recording session, a custom-made tungsten-in-glass microelectrode was set on a micromanipulator (MO-95S, Narishige, Tokyo, Japan). The manipulator was attached to the recording chamber. Extracellular voltage signals were amplified and filtered. Action potentials of single units were isolated online by either a custom-made window-discriminator or a template-matching spike-sorting system (Multi Spike Detector, Alpha-Omega Engineering, Nazareth, Israel). Timings of single-unit discharges were recorded at 1 ms resolution. After the cell's receptive field (RF) was mapped with a small probe stimulus, we presented an RDS that covered the entire RF.

Results

Typical V4 cell responses to cRDS and aRDS are shown in Figure 2. This neuron demonstrates vigorous responses to –0.2° (crossed; 'near' percept) horizontal disparity in cRDS, but not to +0.2° (uncrossed; 'far' percept) disparity (Figure 2). For aRDS, this neuron responded only minimally to either crossed or uncrossed disparities, although slight increases in the discharge rate were visible. The disparity tuning curve for this cell to cRDS exhibits the preference for a range of crossed disparities (filled circles

in Figure 2B). Responses to aRDS did not differ across different disparities (Kruskal-Wallis test, $p > 0.05$). The insensitivity for disparity in aRDS is captured by the flat tuning curve (open squares)
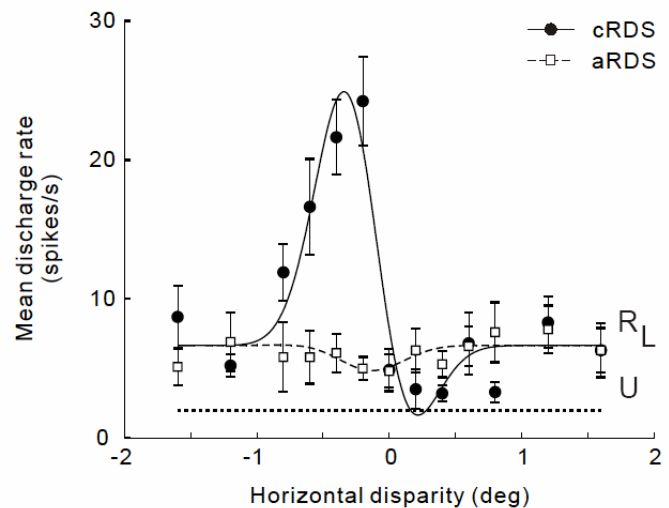
Figure 2. The horizontal disparity-tuning curves to cRDS (solid circles) and aRDS (open boxes) of an example V4 cell. Error bars show the mean ± SEM of 10 trials. The Gabor functions fitted to the raw data points, are superimposed (solid and dashed curves, respectively). The amplitude ratio for this cell was 0.06. The bottom dotted line represents the ongoing activity level, while the mean responses to left- and right-eye monocular presentations are shown on the right-hand side, marked as **L** and **R**, respectively. The **U** mark indicates the mean response to uncorrelated RDS.

We fitted Gabor functions to the disparity tuning curves of all cells that had statistically significant disparity-selectivity either for cRDS or for aRDS (Kruskal-Wallis test, $p < 0.05$; $N = 70$). A Gabor function is given as:

$$R(x) = y_0 + A \cdot e^{\left(-\frac{(x-x_0)^2}{2\sigma^2}\right)} \cdot \cos(2\pi f(x-x_0) + \varphi).$$

The disparity tuning curves to cRDS and aRDS were fit with the four parameters, y_0, x_0, σ, and f, using the same values for both curves. Two parameters, A and φ, were selected independently for the tuning curves for cRDS and aRDS. This function provided a fairly good fit for the disparity tuning in most cells examined, except 11 cells that were discarded in the following analysis.

The ratio of the amplitude parameter, A, between the cRDS disparity tuning curve and the aRDS tuning curve gives a quantitative measure for declines in disparity sensitivity. On the other hand, the inversed profile of the tuning curve would appear as a π shift in the phase, φ. Two-dimensional scatter plots of these two measures of V4 cells indicate that the majority of data points possess amplitude ratio values substantially lower than one (Figure 3A). This result demonstrates that the modulation is reduced to aRDS in most V4 neurons. The median

amplitude ratio was 0.24 (mean, 0.38). A direct comparison with V1 data from a previous study (Cumming & Parker, 1997) shows that the amplitude ratio of V4 cells are significantly lower (Figure 3B, Mann-Whitney test, $p < 0.05$). While phase differences of V1 cells tend to be concentrated near π, phase differences of V4 cells were uniformly distributed from 0 to 2π (χ^2 test, $p > 0.09$).
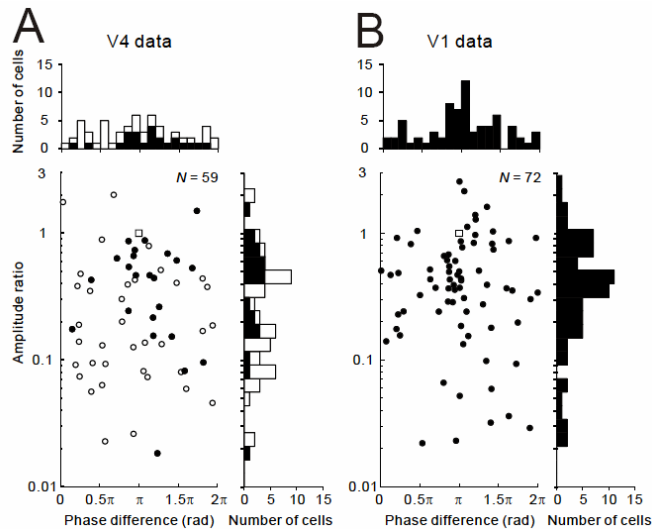
Figure 3. Quantitative analysis of the tuning curve profiles. *A*, Gabor amplitude ratio is plotted against the phase difference between the disparity-tunings to cRDS and aRDS for V4 neurons. The open square indicates where the plot would lie if the responses were perfectly described by the disparity energy model (Ohzawa et al., 1990). The distribution of phase differences and amplitude ratios are plotted in the top and right histograms, respectively. Filled symbols represent cells that have significant disparity sensitivity to both cRDS and aRDS (Kruskal-Wallis test, $p < 0.05$). *B*, The same plots for V1 neurons studied by Cumming & Parker (1997). No statistical test was performed for disparity sensitivity.

Discussion

Analysis of the amplitude of the disparity-tuning curve by fitting the raw data to a Gabor function indicates that the correspondence computation is advanced in V4 (mean amplitude ratio 0.40; median 0.24) in comparison to V1 (mean 0.52; median 0.39; Cumming & Parker, 1997). The reduction of responses to contrast-reversed stimuli is even more prominent in comparison with cat V1 neurons (mean amplitude ratio 0.79; Ohzawa, 1998).

An issue related to the reduction in disparity selectivity for aRDS is possible effects of attention. In an orientation discrimination task, attention increases the amplitude of orientation tuning curve of V4 neurons by a ratio of 1.26 (McAdams & Maunsell, 1999). If the same ratio applies to disparity tuning curves, and attention is always directed toward cRDS and away from aRDS, then our attention-corrected estimate of the mean amplitude ratio is 0.38 x 1.26 = 0.48. Although this is comparable with the mean

amplitude ratio for V1 (0.52; Cumming & Parker, 1997), attentional modulation alone cannot explain the low amplitude ratio observed in V4. While attentional modulation increases with time (McAdams & Maunsell, 1999), the amplitude ratio of V4 cells did not change with time (not shown). We consider it unlikely that attention is a major factor for making the amplitude ratio reduced in V4.

A portion of V1 cells reduces their disparity selectivity when the stimulus is anticorrelated (Cumming & Parker, 1997; Figure 3). Such responses may reflect feedback from higher cortical areas that are responsible for solving the correspondence problem (Ohzawa, 1998). Modification of the disparity energy model without any feedback components, however, can also describe these responses (Read et al., 2002). In V4, rejection of responses to false-matches did not likely result from feedback, because no changes were observed in the response time course. Processing may progressively advance as disparity signals propagate along the visual processing hierarchy, gradually losing the characteristics of the neural responses seen in earlier areas. At the final stage of the ventral visual stream, IT neurons lose their sensitivity to surface concavity and convexity defined by disparity gradients for aRDS (Janssen et al., 2003). These data suggest that the stereo correspondence problem is "fully" solved by the stage of IT. To determine if processing progressively advances along the hierarchy, continuing to advance from V4 to IT, it will be helpful to examine the disparity tuning of IT cells in a similar experimental paradigm.

Conclusion

We found that responses to false-matches are considerably rejected by the stage of V4, raising the possibility that the ventral processing stream may be a neural substrate for global matching computation and the representation of stereoscopic depth. Further studies relating these activities to specific behavior of monkeys performing disparity discrimination tasks should elucidate if neural activity in these areas is functionally involved in stereoscopic depth judgment.

References

Cogan, A.I, Lomakin, A.J., & Rossi, A.F. Depth in anticorrelated stereograms: Effects of spatial density and interocular delay. *Vision Research*, 33, 1959-1975.

Cumming, B.G., & Parker, A.J. 1997 Responses of primary visual cortical neurons to binocular disparity without depth perception. *Nature*, 389, 280-283.

Hinkle, D.A., & Connor, C.E. 2001 Disparity tuning in macaque area V4. *NeuroReport*, 12, 365-369.

Janssen, P., Vogels, R., Liu, Y., & Orban, G.A. 2001 Macaque inferior temporal neurons are selective for three-dimensional boundaries and surfaces. *Journal of Neuroscience*, 21, 9419-9429.

Janssen, P., Vogels, R., Liu, Y., & Orban, G.A. 2003 At least at the level of inferior temporal cortex, the stereo correspondence problem is solved. *Neuron*, 37, 693-701.

Julesz, B. 1971 Foundation of cyclopean perception. Chicago, University of Chicago.

Krug, K., Cumming, B.G., & Parker, A.J. 2004 Comparing perceptual signals of single V5/MT neurons in two binocular depth tasks. *Journal of Neurophysiology*, 92, 1586-1596.

Marr, D., & Poggio, T. 1979 A computational theory of human stereo vision. *Proceedings of the Royal Society of London B Biological Sciences,* 203, 301-328.

McAdams, C.J, & Maunsell, J.H.R. 1999 Effects of attention on orientation-tuning functions of single neurons in macaque cortical area V4. *Journal of Neuroscience*, 19, 431-441.

Ohzawa, I., DeAngelis, G.C., & Freeman, R.D. 1990 Stereoscopic depth discrimination in the visual cortex: Neurons ideally suited as disparity detectors. *Science*, 249, 1037-1041.

Ohzawa, I. 1998 Mechanisms of stereoscopic vision: The disparity energy model. *Current Opinion in Neurobiology*, 8, 509-515.

Poggio, G.F., Motter, B.C., Squatrito, S., & Trotter, Y. 1985 Responses of neurons in visual cortex (V1 and V2) of the alert macaque to dynamic random dot stereograms. *Vision Research*, 25, 397-406.

Read, J.C.A., Parker, A.J., & Cumming, B.G. 2002 A simple model accounts for the response of disparity-tuned V1 neurons to anticorrelated images. *Visual Neuroscience*, 19, 735-753.

Taira, M., Tsutsui, K.I., Jiang, M., Yara, K., & Sakata, H. 2000 Parietal neurons represent surface orientation from the gradient of binocular disparity. *Journal of Neurophysiology*, 83, 3140-3146.

Takemura, A., Inoue, Y., Kawano, K., Quaia, C., & Miles, F.A. 2001 Single-unit activity in cortical area MST associated with disparity-vergence eye movements: Evidence for population coding. *Journal of Neurophysiology*, 85, 2245-2266.

Tanabe, S., Umeda, K., & Fujita, I. 2004 Rejection of false matches for binocular correspondence in macaque visual cortical area V4. *Journal of Neuroscience*, 24, 8170-8080.

Uka, T., Tanaka, H., Yoshiyama, K., Kato, M., & Fujita, I. 2000 Disparity selectivity of neurons in monkey inferior temporal cortex. *Journal of Neurophysiology*, 84, 120-132.

Van Essen, D.C., & Gallant, J.K. 1994 Neural mechanism of form and motion processing in the primate visual system. *Neuron*, 13, 1-10.

Watanabe, M., Tanaka, H., Uka, T., & Fujita, I. 2002 Disparity-selective neurons in area V4 of macaque monkeys. *Journal of Neurophysiology*, 87, 1960-1973.